VARIATIONS OF SOLAR IRRADIANCE, 10.7 cm RADIO FLUX, He I 10830 Å EQUIVALENT WIDTH, AND GLOBAL MAGNETIC FIELD INTENSITY AND THEIR RELATION TO LARGE-SCALE SOLAR MAGNETIC FIELD STRUCTURE*

E. V. IVANOV, V. N. OBRIDKO and I. V. ANANYEV
Institute of Terrestrial Magnetism, Ionosphere, and Radio Wave Propagation, 142092, Moscow region, Russia

(Received 16 October 1996; accepted 12 June 1997)

Abstract. Variations of total solar irradiance, 10.7 cm radio emission, the He I 10830 Å equivalent width and the solar magnetic field flux measured for the entire Sun are compared with variations of the energy index of the global solar magnetic field and the index of the effective solar multipole for years 1979–1992. It is shown that photospheric radiation and that generated in the upper chromosphere and corona display different relationships with the global magnetic field of the Sun, and that interaction between the magnetic field and the solar irradiance is much more complicated than the traditional blocking effect.

1. Introduction

Harvey (1992) compared the total solar magnetic flux measured for the entire Sun with the rotation-averaged values of the total solar irradiance (ACRIM), the 10.7 cm radio flux, the He I 10830 Å equivalent width, and the short-wave radiation in Lα and 1–8 Å X-ray flux. The comparison revealed a different character of the relationship between the magnetic field and the total irradiance coming mainly from the photosphere, on the one hand, and between the magnetic field and chromospheric and coronal radiation, on the other. In this paper we analyze these relationships by comparing the total solar irradiance (SI), the 10.7 cm radio flux (RI), and the He I 10830 Å equivalent width (HeI) with the total solar magnetic flux measured for the entire Sun (MFT), the energy index of the global solar magnetic field $I(B_r)$ and the index of the effective solar multipole (n). We study the crosscorrelation functions of short-term variations of these parameters of the solar irradiance and the total solar magnetic flux.

2. Data Base

In our analysis, we have used daily measurements of the total solar irradiance (SI) from the Nimbus-7, SMM, NASA ERBS, and NOAA-9, 10 satellites, the 10.7 cm

* Paper presented at the SOLERS22 International Workshop, held at the National Solar Observatory, Sacramento Peak, Sunspot, New Mexico, U.S.A., June 17–21, 1996.

Solar Physics **177:** 217–228, 1998.

radio flux data (Ottawa, RI), the equivalent widths of the helium 10830 Å solar absorption line (HeI, in mÅ) averaged over the solar disk (NSO/Kitt Peak), the line-of-sight magnetic field strengths (MFT, in G) measured with 1 arc sec pixels and averaged over the full disk (NSO/Kitt Peak), and the energy index of the global solar magnetic field $(I(B_r))$ and the index of the effective solar multipole, (n), calculated for every rotation during 1979–1992.

The energy index of the global magnetic field, $I(B_r)$, and the index of the effective solar multipole, n, were introduced by Obridko and Ermakov (1989), Obridko and Shelting (1992), Ivanov, Obridko, and Shelting (1997) to characterize the energy and structure of the global magnetic field of the Sun.

$I(B_r) = \langle B^2 \rangle$, on a surface of radius r, where $\langle B^2 \rangle$ is the square intensity of the magnetic field radial component averaged over the solar surface, and r is the radius of the sphere over which the field is averaged. The index was calculated by using the Stanford magnetic maps and their extension in Legendre polynomials performed by Hoeksema (1984).

The index of the effective solar multipole, n, describes the contribution of different components of the global magnetic field at various stages of the 11-year solar cycle:

$$n = -0.5 \log(I_{ss}/I_{ph}) / \log(2.5) \, .$$

It is determined by taking the logarithm of the ratio of the $I(B_r)$ value at the source surface, I_{ss}, to that in the photosphere, I_{ph} (Ivanov, Obridko, and Shelting, 1997). In fact, when passing from the photosphere to the source surface, the magnetic flux changes in accordance with the expression $B_{ss} = B_{ph} r^{-n}$, where $n = 3$ for a dipole source, $n = 4$ for a quadrupole source, and $n > 4$ for a higher-order multipole source. When the field under consideration is a combination of fields from several sources with different weight, n can assume values from 3 to 4 (in the case of combined dipole and quadrupole sources) or higher (in the case of a higher-order multipole field).

3. Processing Methods

Short-term variations of SI, HeI, RI, and MFT were obtained by subtracting the daily SI, HeI, RI, and MFT values, smoothed over 28, 90, and 180 days, from the daily unsmoothed SI, HeI, RI, and MFT values. After that, the cross-correlation functions of the differences obtained – DSI, DHeI, and DRI against DMFT – were calculated for every half-year interval during 1979–1992. The cyclic curves of correlation coefficients and displacements of the main correlation maxima were juxtaposed with the respective cyclic curves of the global magnetic field energy index, $I(B_r)$, and the index of the effective solar multipole, n. Since the cross-correlation functions of DSI, DHeI, and DRI against DMFT, as well as their cyclic

variations proved not to differ very much for different smoothing intervals, we shall only consider variations with a characteristic period of <90 days.

4. Results

4.1. Cross-correlation functions of DSI, DHeI, and DRI against DMFT, and their behavior during a solar cycle

Figure 1(a) illustrates the cross-correlation functions of the short-term variations of SI, RI, and HeI (henceforth denoted as DSI, DRI, and DHeI) against the short-term variations of MFT (denoted as DMFT) for every year from 1979 to 1992. As seen from the figure, the chromospheric (He I 10830 Å equivalent width) and coronal (10.7 cm radio flux) radiations differ from those of mainly photospheric origin (solar irradiance) as far as their relationship with the total solar magnetic flux is concerned. The character of the relationship simplifies when passing from the photosphere to the corona, which can readily be seen from a simpler shape of the correlation function and a weaker dependence on the phase of the cycle. Besides, DRI and DHeI correlate with DMFT, whereas DSI and DMFT in the photosphere display a negative correlation.

The pronounced maximum of the cross-correlation function, corresponding to $\sim$27 days, will be interpreted as evidence of 2-sector structure, and the less pronounced maximum at $\sim 13-14$ days – as evidence of 4-sector structure of the large-scale solar magnetic field. Then in HeI and 10.7 cm, one can readily see 2-sector (and at the growth and decay of the cycle – 4-sector) structures of the large-scale solar magnetic field. Smaller elements are also visible in HeI.

The relationship between DSI and DMFT is much more complicated and changes from year to year. Besides the noticeable minimum near zero, the cross-correlation function has other extreme values that significantly change in their magnitude and position depending on the cycle phase.

Figure 1(b) illustrates the cross correlation between DSI and DMFT for various phases of the solar cycle. At the solar minimum (1985–1986), the character of the relation between DSI and DMFT changes sharply. The cross-correlation minimum shifts from nearly a zero position to about 10–16 days. A more intricate general shape of the cross-correlation function implies a more complicated magnetic field structure and, hence, its specific impact on the emitting elements in the photosphere. The field affects in a different way various structural elements, such as sunspots, plages, and network.

Figure 2 illustrates cyclic variations of the main maximum of the correlation function of DSI, DRI, and DHeI against DMFT at a characteristic variation period of <90 days. The correlation coefficients and shifts were specified by approximating the cross-correlation function in the vicinity of the main maximum of the second-order curve.

The figures imply that:

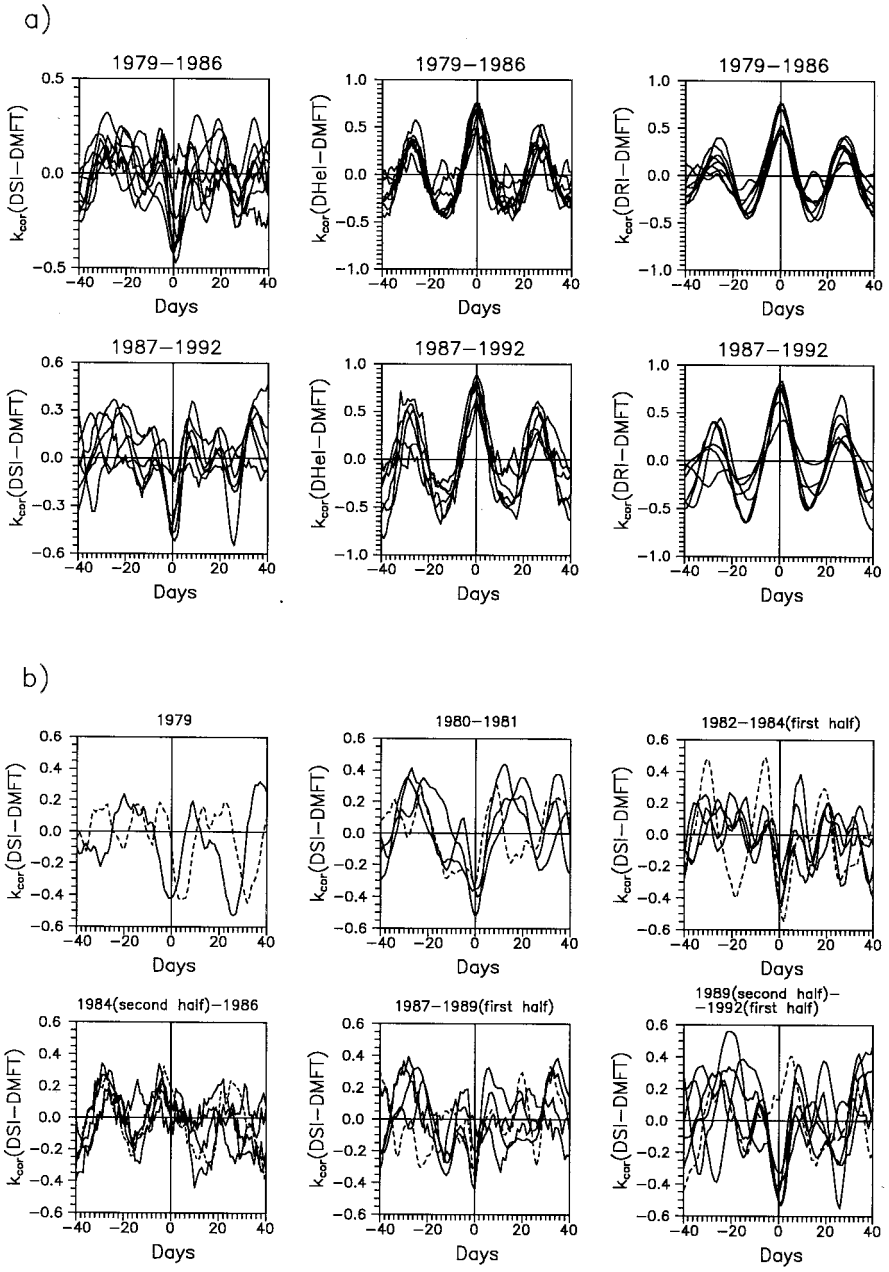

Figure 1. (a) Cross correlations of short-term variations (diurnal minus averaged over 90 days) of the solar irradiance (DSI), He I 10830 Å equivalent width (DHeI), and 10.7 cm radio flux (DRI) with the same short-term variations of the total solar magnetic flux (DMFT) measured over the entire Sun for every year from 1979 to 1992. (b) The same for short-term variations of the solar irradiance (DSI) for every half-year interval from 1979 to 1992 in different phases of the solar cycle. The dashed lines mark the periods of sharp changes of the cross-correlation function (consecutively – second half of 1979, first half of 1981, second half of 1982, second half of 1984, first half 1988, and first half of 1990).

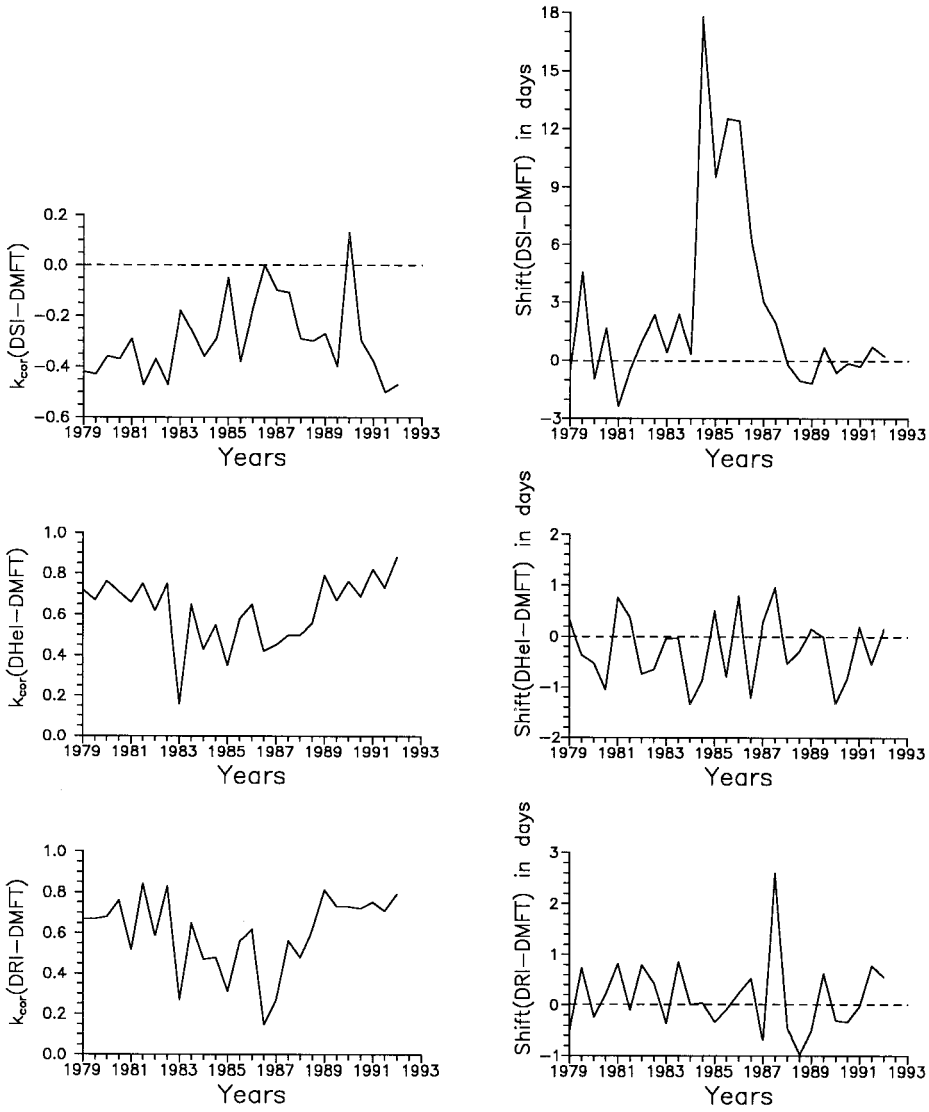

Figure 2. Cyclic variation of the cross correlations and shifts of the short-term variations of SI, HeI, and RI against short-term variations of MFT at a characteristic variation period of <90 days.

(1) The positive correlation of DMFT with DHeI and DRI and the negative correlation with DSI change during the 11-year cycle, the respective correlation and anticorrelation coefficients growing with the solar activity. During most of the cycle (though with a change of phase at the minimum) the DRI−DMFT and DHeI−DMFT curves display a quasi-annual variation of the cross-correlation coefficient. In DSI−DMFT, the variation is also noticeable at the maximum and at the decay of cycle 21.

(2) The main cross-correlation maxima for DSI, DHeI, and DRI as a function of DMFT shift about zero in a different way during the solar cycle:

(a) The shift of DSI relative to DMFT is positive all over the 11-year cycle, except the maximum epochs (1980–1981 and 1988–1991), when it is negative or close to zero (see Figure 2). At the minimum of the cycle (from the second half of 1984 to the second half of 1986), the character of the relationship between SI and MFT changes drastically. The cross-correlation coefficients for the shifts near the zero point are close to 0 or even become positive. At the same time, one can see a noticeable anticorrelation (up to $k_{\text{cor}} = -(0.35–0.40)$ in 1984 and 1985) for the shift of about 10–16 days (see Figure 1(b)).

(b) The shift of DHeI and DRI relative to DMFT changes periodically from positive to negative values with a quasi-period of $\sim$1–2 years during most of the time interval under investigation (1979–1992). It should be noted that the positive shift is more significant for DRI and the negative for DHeI. The shift of DRI with respect to DMFT has a quasi-period of $\sim$1.5 years at the maximum and in the decay phase of cycle 21 and $\sim$2 years at the growth phase and at the maximum of cycle 22. The shift of DHeI about DMFT displays a quasi-biennial variation at the maximum and decay phase of cycle 21 and at the growth phase and maximum of cycle 22. At the minimum of cycle 22, the variation is quasi-annual. The cyclic curves, that describe the correlation of radio emission and HeI radiation with the magnetic field, are very much alike. On the other hand, the shifts in radio emission and HeI behave in an absolutely different way.

4.2. GLOBAL MAGNETIC FIELD INDICES

The global magnetic field of the Sun has a complex hierarchic structure that changes during an 11-year cycle. The hierarchy of solar magnetic fields, from granulation and supergranulation to large-scale systems of giant and supergiant cells (McIntosh and Wilson, 1985; Ivanov, 1986; Abdussamatov, 1993), is most likely due to the multi-layer solar convection. Practically all active events on the Sun are related to one or another of these systems, being concentrated at the cell boundaries, and depending on their dynamics.

To characterize the global magnetic field of the Sun, we have used the energy index of the global magnetic field, $I(B_r)$, and the index of the effective solar multipole, n.

Unlike the total magnetic flux of the Sun (MFT) used by Harvey and White (1996), the $I(B_r)$ index was derived from the sum of the square intensities of the radial field component, rather than from the sum of their absolute values. As a result, more intensive fields contribute to $I(B_r)$ with a bigger weight. Besides, the Stanford maps are obtained with a resolution of $\sim 3'$, whereas the resolution of the NSO/Kitt Peak magnetic maps, used to calculate the total magnetic flux of the Sun, is close to $1''$. Comparison of the cyclic curves for $I(B_r)$ and MFT (Figure 3(a)) shows their similarity. Remove the cyclic trend by subtracting the curve, smoothed over

14 solar rotations, from the cyclic variation. Then the resulting curves (Figure 3(b)) are very similar at the decay phases (1981–1983 and 1990–1991) and display some differences at the maximum and minimum of the 11-year cycle (1980, 1984–1987, and 1989–1990), where the contribution of the intensive fields of sunspots and active regions to MFT and $I(B_r)$ is most significant.

It is shown that the most pronounced maxima on the cyclic curve of the global magnetic field energy index, $I(B_r)$, correspond to the similar maxima on the cyclic curves of different solar activity indices, and coincide with the moments of reconstruction of the large-scale structure of solar magnetic fields and with sharp changes in the solar activity regime as a whole.

Figure 4 illustrates cyclic variation of the index of the effective solar multipole, n, calculated at the source surface ($r = 2.5\ R_0$). As seen from the figure, n changes during the solar cycle (from 3 to 5), which indicates variation of the large-scale solar magnetic field structure. At the growth phase of the cycle, in the epoch of minimum, and in the decay phase, the large-scale structure with characteristic elements $>90^\circ$ (corresponding to a source with $n < 4$) dominates. At the maximum of the cycle, the role of smaller-scale fields ($n > 4$) and their contribution to the total flux increases.

4.3. Relationship between the cyclic curves of correlation coefficients and shifts of DSI, DHeI, and DRI against DMFT, on the one hand, and the cyclic curves of $I(B_r)$ and n indices, on the other

Figures 5 and 6 illustrate cyclic variations of the correlation coefficients and shifts of the cross-correlation functions, DSI, DHeI, and DRI against DMFT, calculated for every half-year interval during 1979–1992, and cyclic variations of the global field indices, $I(B_r)$ and n, smoothed over half-year intervals. Since the correlation coefficients and shift values are calculated at half-year steps, the error in determining the corresponding time moments on the cyclic curves is ± 3 months. Comparison of the curves brings us to the following conclusions:

(1) The cyclic variation of the correlation (or anticorrelation in the case of DSI) coefficients of the functions DSI, DRI, and DHeI against DMFT corresponds on the whole to the cyclic variation of the $I(B_r)$ and n indices, with maximum values at the solar maximum and minimum values at the solar minimum. Quasi-annual and quasi-biennial variations of the correlation (or anticorrelation in case of DSI) coefficients of DSI–DMFT, DHeI–DMFT, and DRI–DMFT functions, on the one hand, and $I(B_r)$ and n indices, on the other, are also synchronous, except for the sign reversal period at the maximum of cycles 21 and 22 (1980, 1990), when the DHeI–DMFT and $I(B_r)$ change in anti-phase. The relation of quasi-annual and quasi-biennial variations of the correlation coefficients of functions DSI–DMFT, DHeI–DMFT, and DRI–DMFT to n is not the same in various phases of the solar cycle and needs further investigation.

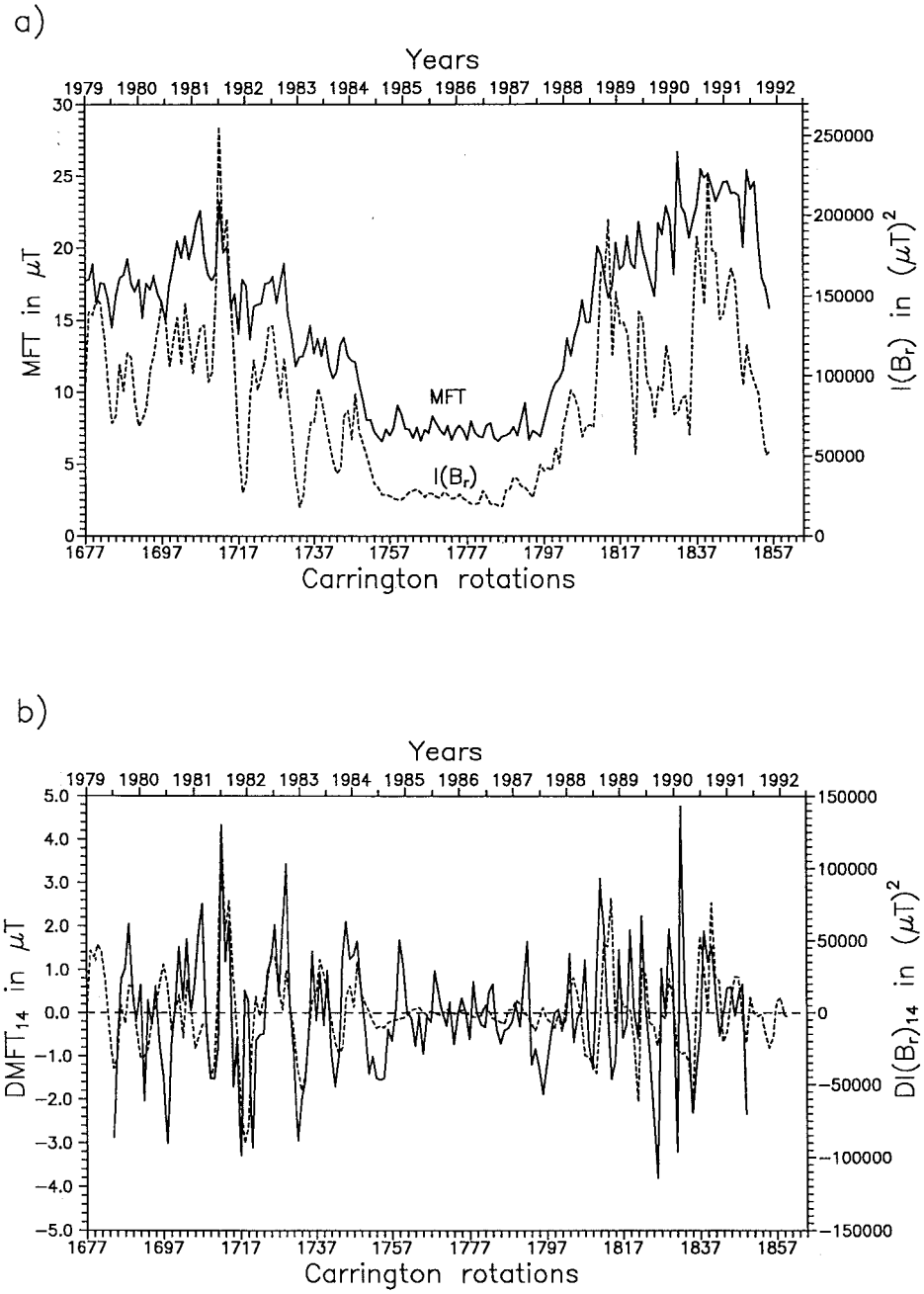

Figure 3. (a) Cyclic variations of the energy index of the global magnetic field $I(B_r)$ and of the rotation-averaged values of the total solar magnetic flux, MFT, measured for the entire Sun for years 1979–1992. (b) The same for $I(B_r)$ and MFT with the cyclic trend removed (obtained by subtracting a curve, smoothed over 14 solar rotations, from the cyclic variation), i.e., $DI(B_r)_{14}$ and DMFT_{14}.

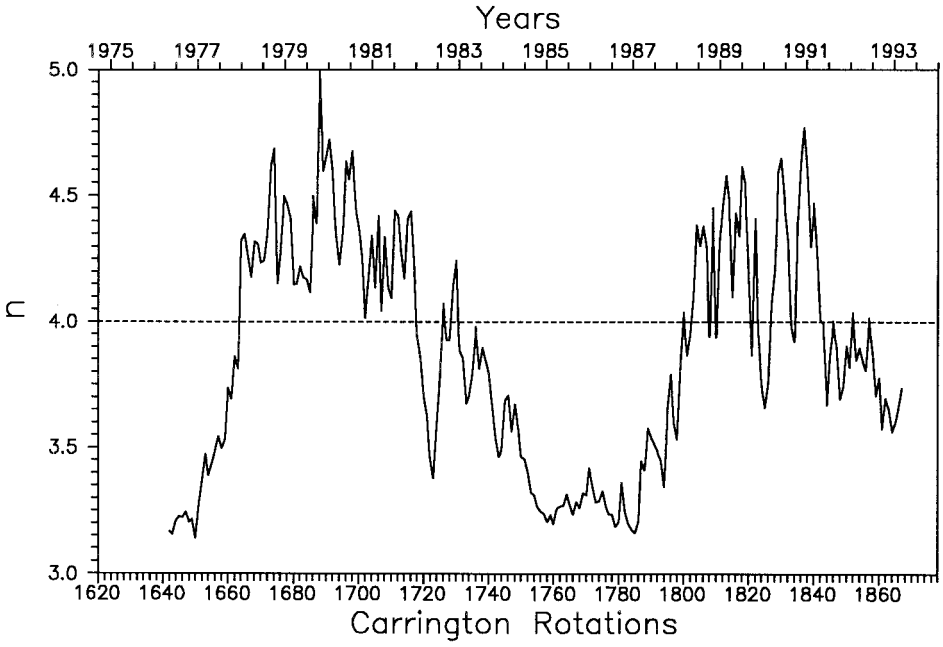

Figure 4. Cyclic variation of the index of the effective solar multipole, n, calculated at the source surface ($r = 2.5\ R_0$) for years 1975–1993.

(2) A cyclic variation of the shift is only detected in the case of DSI: from negative values at the maximum to positive at the minimum of the cycle. DRI and DHeI do not display any systematic shift with the phase of the cycle. We can only state that the negative shift in DRI is larger than the positive one. On the contrary, in the case of DHeI, the positive shift values are larger than negative. Quasi-annual and quasi-biennial variations of the shift reveal the following behavior: (a) anticorrelation in all phases of the cycle for DRI and n, (b) anticorrelation at the maximum and correlation at the growth and decay phases of the cycle for DHeI and n, (c) anticorrelation during cycle 22 and most of cycle 21 for DSI and n. No noticeable dependence is revealed between the shift of the cross-correlation maximum of functions DSI, DHeI, and DRI against DMFT and the $I(B_r)$ index.

5. Conclusions

The study of short-term variations of SI, HeI, and RI as a function of MFT shows that radiations generated in the photosphere (SI) and those generated in the upper chromosphere (HeI) and corona (RI) display a different relationship with the global magnetic field of the Sun (MFT). In both cases, variations are likely to be due to changes in the respective emitting elements, controlled by one or another structure

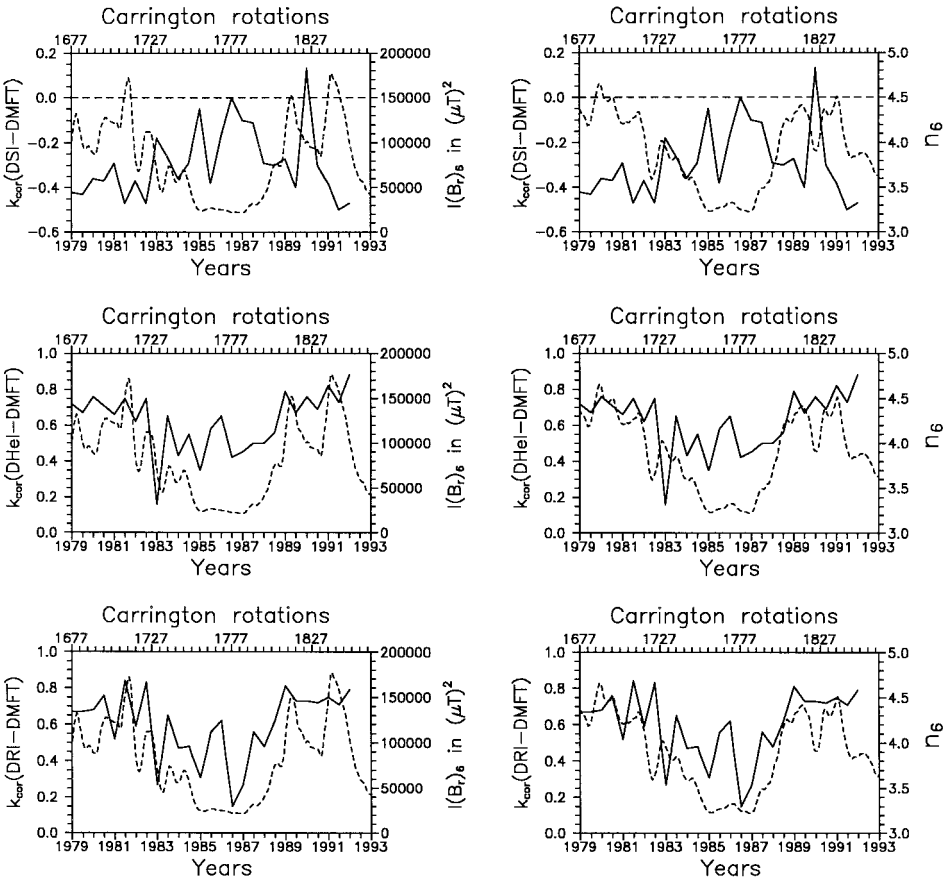

Figure 5. Comparison of cyclic variations of the correlation coefficients of the cross-correlation functions, DSI, DHeI, and DRI versus DMFT (solid curves) (with a characteristic period of <90 days) with cyclic variations of the global field indices, $I(B_r)$ and n (dashed curves), smoothed over half-year intervals, i.e., $I(B_r)_6$ and n_6.

of the global magnetic field of the Sun, as well as to a certain effect of the magnetic field on energy transport in various layers of the solar atmosphere.

The character of cross-correlation functions of short-term variations of SI, HeI, and RI versus MFT implies that the effect of large-scale solar magnetic fields on the structure of the emitting elements grows when passing from the photosphere (SI) to the chromosphere (HeI) and corona (RI). As a result, the index of the large-scale solar magnetic field structure, n, displays the best correlation with RI. If one or another structure of the global magnetic field is determined by the corresponding convection element in the convective layer on the Sun, then the larger the elements of the predominant field structure, and therefore the emitting elements (i.e., the smaller n), the deeper is the base of the corresponding convection layer and the larger is the shift (delay) of the radiation variation relative to variations of the

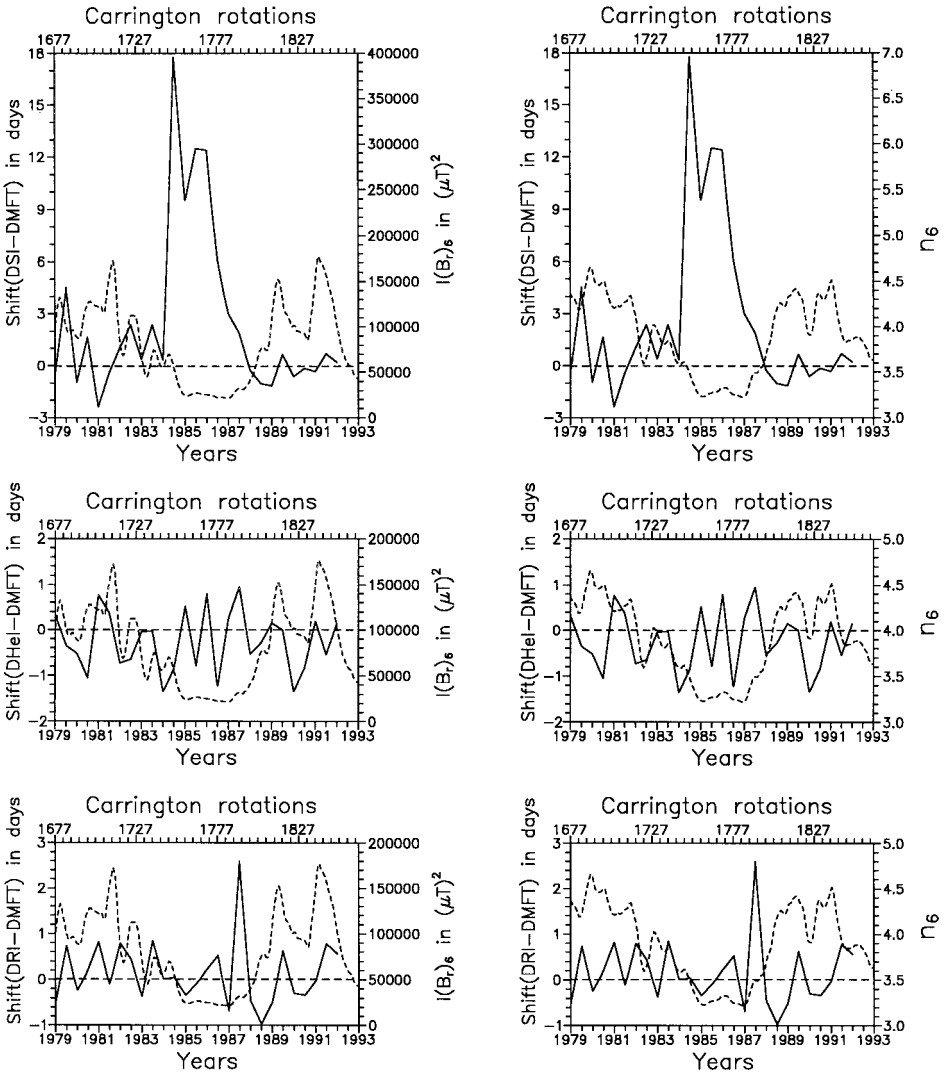

Figure 6. Comparison of the cyclic variations of the shifts of the cross-correlation functions, DSI, DHeI, and DRI versus DMFT (solid curves) (with a characteristic period of $<$90 days) with cyclic variations of the global field indices, $I(B_r)$ and n (dashed curves), smoothed over half-year intervals.

magnetic field of the given structure at its base. If we know the dimensions of elements of the structure that determines this radiation, then the delay time of variations can be used to calculate the propagation velocity of the corresponding wave and to understand its physical nature. The negative shift (outstripping) of the radiation variations relative to the magnetic flux variations is more difficult to interpret. If it is not an artifact, then we must suggest the existence of some mechanism that makes the energy released at the base of the convection layer

propagate ahead of the magnetic field. Thus, interaction between the magnetic field and the solar irradiance is much more complicated that the traditional blocking effect.

Acknowledgements

NSO/Kitt Peak magnetic data used here are produced cooperatively by NSF/NOAO, NASA/GSFC, and NOAA/SEL. The present work was supported by the Russian Foundation for Basic Research (grant No. 06–02–17054).

References

Abdussamatov, H. I.: 1993, *Astron. Astrophys.* **272**, 580.
Harvey, K. L.: 1992, in D. F. Donnelly (ed.), *Proc. of the Workshop on the Solar Electromagnetic Radiation Study for Solar Cycle 22*, U.S. Department of Commerce, SEL NOAA ERL, p. 113.
Harvey, K. L. and White, O. R: 1996, SPRC Technical Report 96-01.
Hoeksema, J. T.: 1984, Ph.D. dissertation, Stanford University.
Ivanov, E. V.: 1986, *Soln. Dannye* No. 7, 61.
Ivanov, E. V., Obridko, V. N., and Shelting B. D.: 1997, *Astron. Reports* **41** (2), 236.
McIntosh, P. S. and Wilson, P. R: 1985, *Solar Phys.* **97**, 59.
Obridko, V. N. and Ermakov, F. A.: 1989, *Astron. Circ.* **1539**, 24.
Obridko, V. N. and Shelting, B. D.: 1992, *Solar Phys.* **137**, 167.